

Multimode Transport in Schottky-Barrier Carbon-Nanotube Field-Effect Transistors

J. Appenzeller,¹ J. Knoch,² M. Radosavljević,¹ and Ph. Avouris¹

¹*IBM T.J. Watson Research Center, Yorktown Heights, New York 10598, USA*

²*Institut für Schichten und Grenzflächen, Forschungszentrum Jülich, D-52425 Jülich, Germany*

(Received 21 January 2004; published 4 June 2004)

We present a detailed study on the impact of multimode transport in carbon nanotube field-effect transistors. Under certain field conditions electrical characteristics of tube devices are a result of the contributions of more than one one-dimensional subband. Through potassium doping of the nanotube the impact of the different bands is made visible. We discuss the importance of scattering for a stepwise change of current as a function of gate voltage and explain the implications of our observations for the performance of nanotube transistors.

DOI: 10.1103/PhysRevLett.92.226802

PACS numbers: 73.63.-b, 73.22.-f, 73.23.-b, 72.10.-d

Since it was first shown that single wall carbon nanotubes (CNs) can operate in a conventional field-effect transistor (FET) mode [1,2], the electrical characteristics of CNFETs have been significantly improved particularly by increasing the gate field impact [3–5]. One goal of these studies is to evaluate the potential of ultimately scaled nanotube devices for future electronic applications. This effort is accompanied by the development of suitable models to predict the electrical characteristics of nanotube transistors [6–8]. Models describing the experimental observations best include Schottky barriers (SBs) at the metal contact-nanotube interface [9,10] and assume ballistic transport conditions inside the tube. In fact, recent experiments indicate that transport in semiconducting nanotubes is ballistic over distances of at least a couple of hundred nanometers at room temperature [11–13]. In addition, it is typically assumed that only one one-dimensional (1D) mode in the nanotube is involved in current transport. In this Letter we discuss to what extent the last assumption is justified and how the number of modes—1D subbands—involved impacts the device characteristics.

Nanotube band structures have been studied extensively in the past through theory and experiment. Scanning tunneling spectroscopy [14,15] and absorption spectroscopy [16] have been used to map the density of states in various nanotube samples. Most of the insights gained are related to the lowest conduction/valence band and correspondingly to the energy gap in the case of semiconducting nanotubes. Tight binding (TB) calculations are in reasonable agreement with such experiments. From TB one may also infer that higher subbands are separated by several hundred meV from the lowest 1D bands with the exact value depending on the tube chirality [17]. For tubes produced by laser ablation [18] as those used in this Letter with a diameter of $t_{\text{ch}} \approx 1.4$ nm, the separation between the lowest conduction band and the next 1D subband is expected to be around ~ 270 meV from spectrofluorimetric measurements [17]. On the other hand, in a CNFET the applied drain or gate voltages (V_{ds} and V_{gs} , respectively) usually exceed half a volt, and it is

important to investigate whether higher modes are involved in the CNFET transport properties under particular voltage conditions.

One may argue that higher bands should result in certain features in the electrical characteristics of CNFETs. For example, the drain current I_{d} as a function of V_{gs} may be expected to increase stepwise due to the quantized conductance contributions $G = 4e^2/h$ of individual 1D modes [19]. We will show here that the absence of any particular structure in the electrical characteristics of CNFETs is no proof of pure one-mode transport and that particular care has to be taken when CNFET data are analyzed within a one-band model.

CNFETs were fabricated on a silicon substrate that acts as a common gate. A thin layer of silicon dioxide $t_{\text{ox}} = 5$ nm isolates the conducting silicon from the semiconducting tube channel. The source/drain separation is around $L = 300$ nm. Contacts are made of titanium. Tubes are spun on the substrate prior to source/drain definition. Details of the sample fabrication can be found elsewhere [20]. All measurements were performed at room temperature in a vacuum chamber.

Prior to any particular treatment electrical characteristics show a typical p -type behavior [21]. This means that substantial currents in the on state of the transistor are obtained only for sufficiently negative gate voltages V_{gs} . Through potassium doping of the entire tube n -type characteristics can be obtained [22]. The inset of Fig. 1 shows representative transfer characteristics $I_{\text{d}}(V_{\text{gs}})$ of a potassium doped nanotube for drain voltages between +0.1 and +0.5 V. The threshold voltage V_{th} , the gate voltage for which the device starts to turn on, is approximately -0.8 V. Increasing the amount of potassium deposited in vacuum on the nanotube results in a continuous shift of V_{th} towards more negative values up to a maximum of $V_{\text{th}} \approx -1.5$ V. At this high doping level CNFET characteristics consistently develop an unusual steplike change of current as a function of gate voltage as shown in Fig. 1. Instead of a monotonic current increase up to a maximum value that is given by the details of the contact resistance, $I_{\text{d}}(V_{\text{gs}})$ saturates for certain V_{gs} ranges.

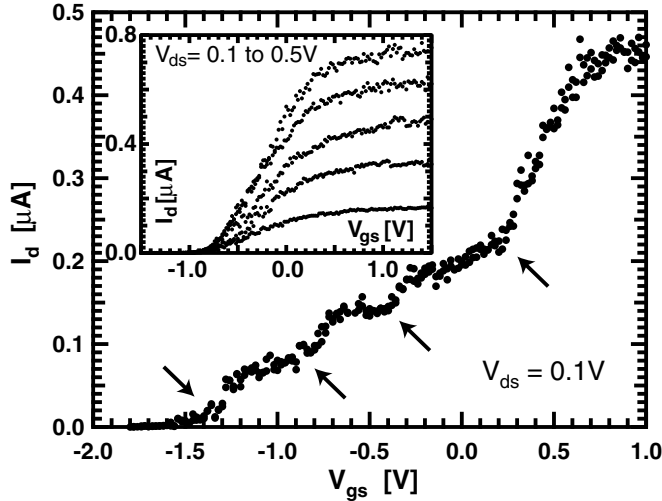


FIG. 1. Current as a function of V_{gs} at $T = 300$ K for a heavily K -doped CNFET. The onset of higher bands is marked by arrows. The inset shows transfer characteristics for the same tube FET after light K doping.

We argue that this unusual behavior is a result of the stepwise increase of current carrying 1D modes in the tube when V_{gs} is increased (made more positive for an n -type FET). However, current saturation *does not* occur below the quantum limit ($I \sim G = 4 e^2/h$) if transport in the channels is ballistic. This means that the superposition of contributions from bands *without* scattering results in a smooth increase in current. To explain the observed steplike behavior we have to assume that scattering inside the nanotube results in a saturation of the current carrying capability of every 1D band. In our case a sufficiently high doping level ensures a small enough transmission through the nanotube channel. This means that the contributions from different 1D bands can be made visible through the introduction of scattering sites. Within this context it also becomes clear why Antonov and Johnson [23] observed steps in their measurements *only* in the presence of an impurity and why the same steps are not present for most CNFETs.

We will now discuss the details of the picture we propose and describe how we have modeled the situation in a diffusive Schottky barrier CNFET. Figure 2 illustrates the situation in a SB transistor under certain drain and gate voltage conditions if scattering is enabled. We have employed the nonequilibrium Green function formalism [24] to calculate the charge in and the current through the nanotube channel. A self-consistent solution is achieved by iteratively solving the modified Poisson equation together with the equations for the Green function. Scattering is introduced according to Ref. [25] by attaching independent Büttiker probes to each site of the underlying finite difference grid. One probe is attached to every grid point sharing a common Fermi level. This Fermi level represents the quasi-Fermi level inside the channel at this particular position and is determined

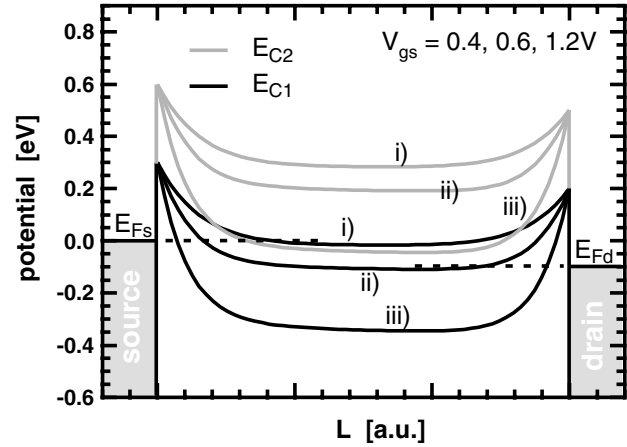


FIG. 2. Band bending situation in a CNFET for $V_{ds} = 0.1$ V. Here $\Delta E_{C1-C2} = 0.3$ eV, and $l_s = 1/30L$ has been assumed. Curves (i)–(iii) indicate the situation for the first and second subband (black and gray) for three different V_{gs} .

self-consistently by making the total current contribution of the probes zero at every grid point. Thus, intrasubband as well as intersubband scattering is taken into account. The coupling strength between probe and channel is described by a parameter α that can be varied between one and zero. α is a means to define the scattering probability inside the tube channel and can be directly related to a characteristic scattering length l_s [25]. As illustrated by Fig. 2, the higher the V_{gs} the thinner the Schottky barrier at the source and drain contacts and the lower the bands in the bulk portion (the middle part) of the nanotube. Scattering results in a continuous voltage drop (a slight tilt of the bands towards the lower right) inside the tube. Moreover, our simulations do not indicate that the band movement stops with increasing V_{gs} as typically observed for a conventional metal-oxide-semiconductor field-effect transistor (MOSFET). This observation is consistent with the notion that the gate voltage for CNFETs operating near the quantum capacitance limit controls the potential rather than the charge and is, in particular, a consequence of the 1D density of states in a tube. It is this fact that enables the second band (gray) to bend down sufficiently to allow current injection into it.

Next we discuss the details of the gate impact on the current through a CNFET and relate the band bending situations (i)–(iii) in Fig. 2 to characteristic aspects of the $I_d(V_{gs})$ curve. Figure 3(b) shows the calculated current through a nanotube FET as a function of V_{gs} . At (i), $V_{gs} \approx V_{th}$, the device starts to turn on since the Fermi level in source E_{Fs} coincides approximately with the first conduction band E_{C1} inside the bulk portion of the nanotube. A substantial tunneling current can be injected into the device similar to the ballistic case discussed elsewhere [7]. Upon increasing V_{gs} the current increases by improving the coupling between the electron reservoirs in source and drain through thinning of the Schottky barriers. At

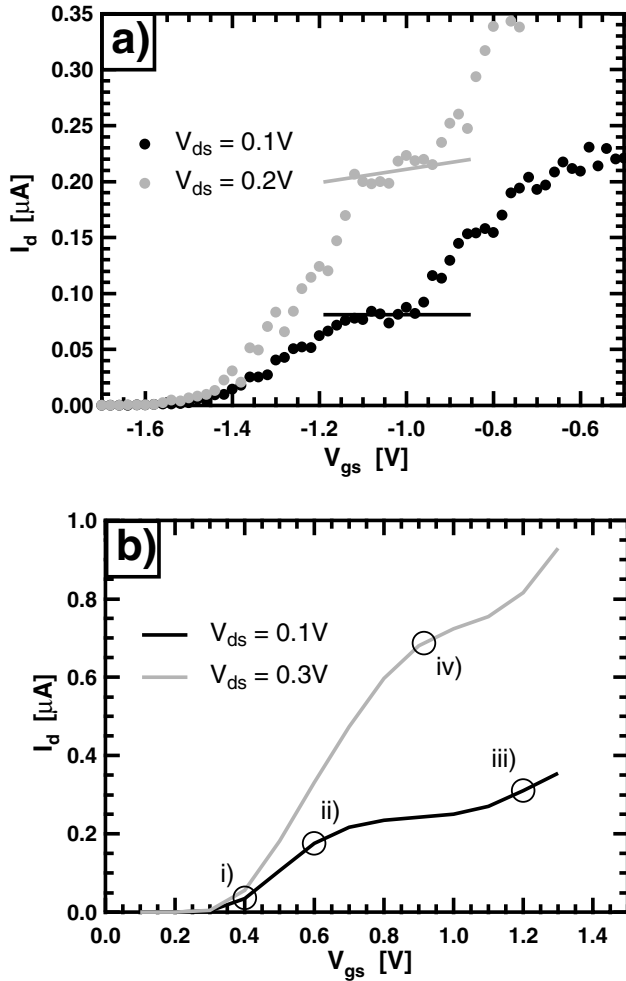


FIG. 3. Experimental (a) and theoretical (b) results on the V_{gs} response of a highly doped SB CNFET for different V_{ds} . (i)–(iii) correlate to the band bending situations in Fig. 2. (iv) corresponds to (ii) for a higher V_{ds} .

(ii) both barriers are transparent enough such that the device resistance is dominated by scattering inside the diffusive nanotube channel—a situation that does not occur in an undoped ballistic SB CNFET. For a gate voltage independent scattering rate, as assumed here, and a constant drain voltage, increasing V_{gs} further does not alter the channel resistance. This situation is different from a two-dimensional (2D) system as a conventional MOSFET where increasing the carrier concentration inside the channel by means of V_{gs} typically results in an increase of I_d . The key factor here is the 1D character of the nanotube. In the case of a ballistic channel, increasing the gate voltage increases the velocities $v_F(E)$ of carriers at the quasi-Fermi level inside the tube. However, at the same time, the number of electrons actually involved in current transport decreases due to the energy dependence of the 1D density of states $D_{1D}(E)$. The product $D_{1D}(E) \cdot v_F(E)$ remains constant. Scattering changes this picture only in so far that the current level

for which saturation occurs is reduced. Finally, in case (iii), when the second subband (gray) reaches E_{FS} , a new cycle starts, another channel for current transport opens up and I_d starts increasing again up to the next plateau. Steps are equal only in height if scattering in different 1D bands is identical. For larger V_{gs} (case iv) current saturation occurs at a level that roughly scales linearly with V_{ds} and steps become less prominent. Figure 3(a) shows experimental results for another highly doped CNFET sample at two drain voltages. Note that V_{th} for this n -type device is around -1.5 V due to the high doping level, while in our simulation we did not try to accommodate for a doping related V_{th} shift. The general agreement between simulation and experiment is apparent.

Having identified the basic physics behind the occurrence of the stepwise increase of I_d as a function of V_{gs} we can now use our measurement to extract information about the nanotube band structure. The gate voltage difference ΔV_{gs} between (i) and (iii) is a measure of the energy difference $\Delta E_{C_n-C_{n+1}}$ between two 1D bands. For a gate oxide thickness of 5 nm, we extract from our simulation that $\Delta E_{C_n-C_{n+1}} \approx 0.5\Delta V_{gs}$. Accordingly, we conclude that in the case of Fig. 1 the energy separation between the first and second, the second and third, and the third and fourth 1D bands are approximately 275, 225, and 300 meV, respectively. Similar results were obtained for tubes treated the same way [see, e.g., Fig. 3(a)]. While $\Delta E_{C_1-C_2} \approx 275$ meV compares well with the expected TB value of ~ 270 meV for the types of tubes used here [17], $\Delta E_{C_2-C_3} \approx 225$ meV is significantly smaller than anticipated. This shows that the nanotube band structure $E(k)$ has been substantially affected by the extensive potassium doping as suggested by theory [26] and is, to the best of our knowledge, the first experimental observation of this particular behavior.

Finally, we focus on the implications of our findings for experiments on CNFETs that do not exhibit a stepwise change in current due to the absence of scattering sites. Figure 4 displays $\log I_d(V_{gs})$ for the *same* CNFET for two distinct doping levels at drain voltages of 0.1, 0.3, and 0.5 V, respectively. Curves for the lightly doped case (gray) are offset by $\Delta V_{th} \sim -0.66$ V to help the comparison. At around $V_{gs} = -0.3$ V for $V_{ds} = 0.1$ V the onset of a second subband can be deduced from the heavily doped sample (black). Since the similarity between measurements in the deep subthreshold regime ($V_{gs} \leq -1$ V) at different K levels is apparent, it is reasonable to assume that also in the lightly doped case (gray) more than one subband is involved in current transport at high positive gate voltages. Contributions from higher subbands, however, are invisible and become apparent only if scattering inside the channel is strong enough to limit the current carrying capability per subband substantially. The nonexistence of any pronounced features in CNFET characteristics is thus no proof of one-mode transport.

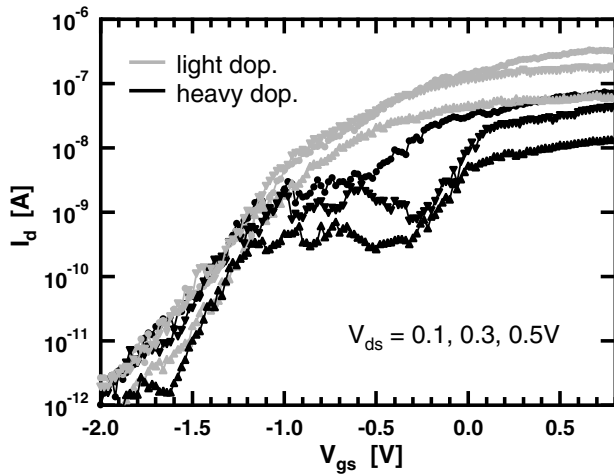


FIG. 4. $\log I_d(V_{gs})$ for a CNFET at two different doping levels for $V_{ds} = 0.1, 0.3, \text{ and } 0.5 \text{ V}$.

Recently, very high current levels have been reported for CNFETs at substantial gate voltage overdrives $V_{gs} - V_{th} > 3.5 \text{ V}$ [27]. Transistors consist of tubes with diameters of around $t_{ch} \approx 2.5 \text{ nm}$ on a 10 nm gate oxide. From our experimental and simulation results we conclude that for the highest V_{gs} used in the experiments by Javey *et al.* [27] at least three 1D modes are involved in current transport when taking into account the expected mode spacing for the type of tubes used. As stated above, the absence of strong backscattering for small V_{gs} prevents the simple observation of the multimode transport conditions but does not prevent its impact on the electrical characteristics. This is an important finding since it implies that conductance values $G > 4 e^2/h$ should be observable in the linear regime of the CNFET output characteristics. It is also of relevance for the extraction of SB heights at the metal nanotube interfaces. A detailed quantitative analysis of CNFET data should take more than one 1D mode into account.

In summary, we have investigated the impact of multimode transport in CNFETs on the electrical characteristics of the same. While no stepwise change in current as a function of V_{gs} may be observed due to a small or vanishing scattering probability inside the tube, more than one subband can be involved in current transport for high V_{gs} . Experimentally, subbands have been made visible through extensive doping with potassium. A model has been presented to explain our results consistently, and the implications of our findings for electrical characteristics of CNFETs have been discussed.

[1] S.J. Tans, A. Verschueren, and C. Dekker, *Nature (London)* **393**, 49 (1998).

- [2] R. Martel, T. Schmidt, H.R. Shea, T. Hertel, and Ph. Avouris, *Appl. Phys. Lett.* **73**, 2447 (1998).
- [3] A. Bachtold, P. Hadley, T. Nakanishi, and C. Dekker, *Science* **294**, 1317 (2001).
- [4] A. Javey, H. Kim, M. Brink, Q. Wang, A. Ural, J. Guo, P. McIntyre, P. McEuen, M. Lundstrom, and H. Dai, *Nature Materials* **1**, 241 (2002).
- [5] S. Wind, J. Appenzeller, R. Martel, V. Derycke, and Ph. Avouris, *Appl. Phys. Lett.* **80**, 3817 (2002).
- [6] F. Leonard and J. Tersoff, *Phys. Rev. Lett.* **88**, 258302 (2002).
- [7] J. Appenzeller, J. Knoch, R. Martel, V. Derycke, S. Wind, and Ph. Avouris, *IEEE Trans. Nanotechnol.* **1**, 184 (2002).
- [8] J. Guo, S. Datta, and M. Lundstrom, *IEEE Trans. Electron Devices* **51**, 172 (2004).
- [9] S. Heinze, J. Tersoff, R. Martel, V. Derycke, J. Appenzeller, and Ph. Avouris, *Phys. Rev. Lett.* **89**, 106801 (2002).
- [10] J. Appenzeller, J. Knoch, V. Derycke, R. Martel, S. Wind, and Ph. Avouris, *Phys. Rev. Lett.* **89**, 126801 (2002).
- [11] S. Wind, J. Appenzeller, and Ph. Avouris, *Phys. Rev. Lett.* **91**, 058301 (2003).
- [12] A. Javey, J. Guo, Q. Wang, M. Lundstrom, and H. Dai, *Nature (London)* **424**, 654 (2003).
- [13] T. Dürkop, S. A. Getty, E. Cobas, and M. S. Fuhrer, *Nano Lett.* **4**, 35 (2004).
- [14] J.W.G. Wildoer, L.C. Venema, A.G. Rinzler, R.E. Smalley, and C. Dekker, *Nature (London)* **391**, 59 (1998).
- [15] T.W. Odom, J.L. Huang, P. Kim, and C.M. Lieber, *Nature (London)* **391**, 62 (1998).
- [16] A. Hagen and T. Hertel, *Nano Lett.* **3**, 283 (2003).
- [17] S.M. Bachilo, M.S. Strano, C. Kittrell, R.H. Hauge, R.E. Smalley, and R.B. Weisman, *Science* **298**, 2361 (2002).
- [18] A. Thess, R. Lee, P. Nikolaev, H. Dai, P. Petit, J. Robert, C. Xu, Y.H. Lee, S.G. Kim, A.G. Rinzler, D.T. Colbert, G.E. Scuseria, D. Tomanek, J.E. Fischer, and R.E. Smalley, *Science* **273**, 483 (1996).
- [19] J. Guo, M. Lundstrom, and S. Datta, *Appl. Phys. Lett.* **80**, 3192 (2002).
- [20] S. Wind, M. Radosavljevic, J. Appenzeller, and Ph. Avouris, *J. Vac. Sci. Technol. B* **21**, 2856 (2003).
- [21] Ph. Avouris, J. Appenzeller, R. Martel, and S. Wind, *Proc. IEEE* **91**, 1772 (2003).
- [22] M. Bockrath, J. Hone, A. Zettl, P.L. McEuen, A.G. Rinzler, and R.E. Smalley, *Phys. Rev. B* **61**, R10606 (2000).
- [23] R.D. Antonov and A.T. Johnson, *Phys. Rev. Lett.* **83**, 3274 (1999).
- [24] S. Datta, *Electronic Transport in Mesoscopic Systems* (Cambridge University, Cambridge, England, 1995).
- [25] R. Venugopal, M. Paulsson, S. Goasguen, S. Datta, and M.S. Lundstrom, *J. Appl. Phys.* **93**, 5613 (2003).
- [26] Ch. Jo, Ch. Kim, and Y.H. Lee, *Phys. Rev. B* **65**, 035420 (2002).
- [27] A. Javey, Q. Wang, W. Kim, and H. Dai, *IEDM Technical Digest* **2003**, 741 (2003).